PCCP

Understanding surface charge regulation in silica nanopores

Journal:	*Physical Chemistry Chemical Physics*
Manuscript ID	CP-ART-04-2020-002152
Article Type:	Paper
Date Submitted by the Author:	22-Apr-2020

Complete List of Authors:	Yang, Jie; East China University of Science and Technology, School of Chemistry and Molecular Engineering Su, Haiping; East China University of Science and Technology Lian, Cheng; State Key Laboratory of Chemical Engineering, East China University of Science and Technology., ; East China University of Science and Technology School of Chemistry and Molecular Engineering, Shang, Yazhuo; East China University of Science and Technology, Chemistry Liu, Honglai; East China University of Science and Technology, Wu, Jianzhong; University of California, Riverside, Chemical and Environmental Engineering

Understanding surface charge regulation in silica nanopores

Jie Yang[1], Haiping Su[1], Cheng Lian[1,2*], Yazhuo Shang[1], Honglai Liu[1*] and Jianzhong Wu[3*]

[1]State Key Laboratory of Chemical Engineering, Shanghai Engineering Research Center of Hierarchical Nanomaterials, and School of Chemistry and Molecular Engineering, East China University of Science and Technology, Shanghai 200237, China

[2]Institute for Theoretical Physics, Center for Extreme Matter and Emergent Phenomena, Utrecht University, Princetonplein 5, 3584 CC Utrecht, The Netherlands

[3]Department of Chemical and Environmental Engineering, University of California, Riverside, CA 92521, USA

Abstract: Nanoporous silica is used in a wide variety of applications, ranging from bioanalytical tools and materials for energy storage and conversion as well as separation devices. The surface charge density of nanopores is not easily measured by experiment yet plays a vital role in the performance and functioning of silica nanopores. Herein, we report a theoretical model to describe charge regulation in silica nanopores by combining the surface-reaction model and the classical density functional theory (CDFT). The theoretical predictions provide quantitative insights into the effects of pH, electrolyte concentration, and pore size on the surface charge density and electric double layer structure. With a fixed pore size, the surface charge density increases with both pH and the bulk salt concentration similar to that for an open surface. At fixed pH and salt concentration, the surface charge density rises with the pore size until it reaches the bulk asymptotic value when the surface interactions become negligible. At high pH, the surface charge density is mainly determined by the ratio of the Debye screening

*Email: liancheng@ecust.edu.cn (C.L.), hlliu@ecust.edu.cn (H.L.), jwu@engr.ucr.edu(J.W.)

length to the pore size (λ_D/D).

Keywords: nanoporous silica, surface charge regulation, CDFT, electric double layer

1 Introduction

Recent progress in nanotechnology enables various applications of nanoporous silica such as bioanalytical tools[1,2,3], separation devices[4], or energy conversion/storage.[5,6] Its broad applicability is owing to high surface area, tunable pore size, biocompatibility, and chemical stability. The surface charge of nanoporous silica is mostly negative due to protonation/deprotonation of the dissociable functional groups at the solid interface.[7,8] It has been generally recognized that the electrophoretic behavior of nanoporous silica depend on their surface charge densities, which vary with the solution conditions[9] and the pore sizes.[9,10]

Several investigations have been attempted to characterize the surface charge density of silica nanopores through experiment. Electrokinetic techniques including streaming potential or electrophoresis analysis mostly focused on the electrical surface potential (zeta potential). [9-13] However, the interpretation of such experiments is problematic when the electrical double layers within the nanopore are highly overlapped. The problem arises mainly due to the data analysis based on the Helmholtz-Smoluchowski and the Gouy-Chapman equations that are unreliable for such systems.[14,15] Another method to estimate the surface charge is through potentiometric titration by monitoring the number of ions and protons absorbed at the interface of nanoporous silica.[16-20] Even though the charge density and the local ionic composition remain elusive, it provides a quantitative connection between ion adsorption and the regulation of the surface charge.

Theoretical modeling provides a valuable alternative to experimental investigation of the surface charge regulation mechanism for nanoporous silica.[21] Conventional methods based on Poisson-Boltzmann (PB) or the Poisson-Nernst-Planck (PNP) equations have been widely used due to their high efficiency in describing the electrical double layer and electroosmotic flows.[22-27] Recent studies provided the pore level analysis on the mesoporous internal surface charge at various porosities and ionic conditions.[28,29] However, the conventional methods ignore the ionic volume exclusion effects and electrostatic correlations important for concentrated electrolytes in nanoscale pores.[30,31] Such effects should be considered to understand the charge regulation of silica nanopore under nanoconfinement.

Increasing studies suggest that classical density functional theory (CDFT) is able to describe various equilibrium and transport properties of confined ionic systems including electrolytes in nanoscale porous materials.[32-37] In this work, we combine CDFT with a surface reaction model to investigate the effects of pH, electrolyte concentration, and pore size (as small as 1 nm) on the surface charge density of porous silica. Whereas disordered porous silica has a complex pore size distribution and diverse pore shapes, theoretical investigations in this work are focused on a slit pore model that intends to capture the essential features of realistic porous silica submerged in electrolytes. The theoretical results show the significant role of the pore size in determining the surface charge density, in particular when it is in the range of the Debye screening length. The remaining of this paper is structured as follows. First, we recapitulate the thermodynamic and kinetic models and the computational scheme underpinning the CDFT and the surface-equilibrium calculations. The technical details can be found in our previous publications.[38,39] Next, we discuss the theoretical predictions on the pH,

66 salt concentration, and pore size effects on the surface charge density of various silica
67 nanopores. Finally, we summarize the results. The single silt pore modeling methods could be
68 further integrated with other theories such as effective medium approximation (EMA)[30] for
69 understanding the charge regulation of more realistic porous silica in the future, which would
70 provide implications for possible applications.

71 **2 Model and methods**

72 ***2.1 Theoretical model***

73 We consider a generic model for a silica nanopore as shown schematically in Figure 1a.
74 The nanopore is submerged in an aqueous electrolyte solution with various ionic species
75 (throughout this work, subscript i = 1 stands for H^+, i = 2 for Na^+, i = 3 for Cl^-, and i = 4
76 for OH^-). As explained in the next subsection, we use the restricted primitive model to
77 investigate the effects of the pore size, electrolyte concentration, and pH on the surface
78 properties of nanoscale silica pores. Figure 1b and 1c show schematically how the surface
79 charge density and the surface electrical potential (zeta potential) are determined by a
80 combination of the electric double layer (EDL) and the surface-reaction models.

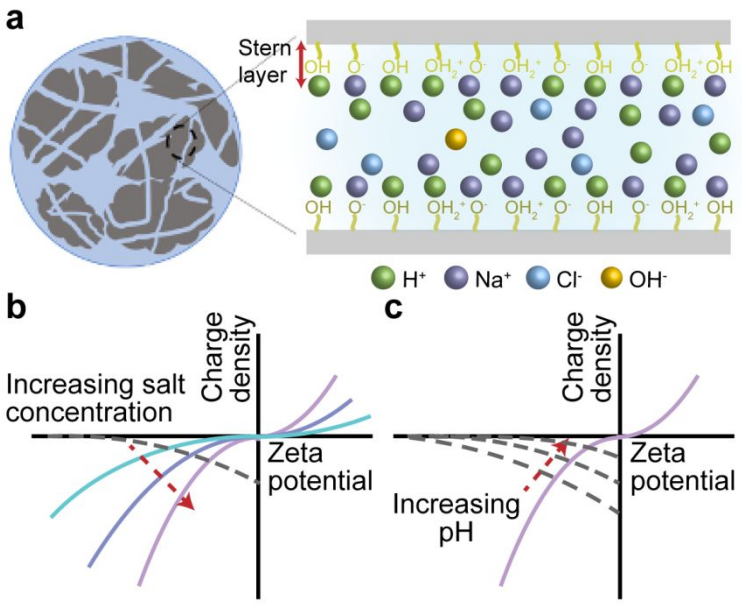

Figure 1. (a) Schematic of the functional groups and the electrical double layer (EDL) in a silt pore of porous silica submerged in an electrolyte solution. Panels b and c illustrate how, at a fixed salt concentration and a fixed pH, respectively, the surface charge density and the zeta (surface) potential are determined by the interception of the corresponding curves predicted by the EDL (solid lines) and the surface reaction models (dashed lines).

2.2 CDFT for electric double layers

Ion distributions in silica nanopores are described with the restricted primitive model (RPM) of electrolyte solutions. Both cations and anions are represented by charged hard spheres of the same size since the hydrated radius of sodium and chloride are similar to each other.[40] While atomic details are neglected, the primitive model is able to account for electrostatic correlations and mean ionic excluded volume effects important for understanding charge regulation. According to this model, the pair ionic potential is given by

$$\mu_i = \begin{cases} \infty, & r < (\sigma_i + \sigma_j)/2 \\ Z_i Z_j e^2/(4\pi\varepsilon_0\varepsilon_r r), & r \geq (\sigma_i + \sigma_j)/2 \end{cases} \quad (1)$$

where r is the center-to-center distance between ions, e is the elementary charge, ε_r is the solvent dielectric constant, ε_0 is the permittivity of the free space, σ_i and Z_i are the hard-

sphere diameter and the valence of ionic species i, respectively. In our CDFT calculations, both anions and cations are assumed to be monovalent, the diameter of all particles (solvated ions) is fixed at $\sigma = 0.3\,nm$, and the dielectric constant for liquid water is $\varepsilon_r = 78$.[41] In consistent with the primitive model, the silica nanopore is represented by the slit model with pore width D and uniform surface charge density Q. The non-electrical component of interaction between the silica nanopore and ion species i is modeled as a hard-wall potential $V_i(z)$

$$V_i(z) = \begin{cases} \infty, z \le \frac{\sigma_i}{2} \text{ or } z \ge D - \frac{\sigma_i}{2} \\ 0, \text{otherwise} \end{cases} \quad (2)$$

where the z is the perpendicular distance from the pore surface.

At given temperature T and bulk ion concentrations $\rho_i^0(z)$, CDFT predicts that the ionic density distributions inside the pore are given by

$$\rho_i(z) = \rho_i^0 \exp\left[-\beta V_i(z) - \beta Z_i e\psi(z) - \beta\,\Delta\mu_i^{ex}(z)\right] \quad (3)$$

where $\beta = 1/(k_B T), T = 300\,K$, k_B is the Boltzmann constant, and $\Delta\mu_i^{ex}(z)$ accounts for electrostatic correlations and ionic excluded volume effects. The detailed equation for the local chemical potential can be found in our previous publications.[38,39]The mean electric potential, $\psi(z)$, is related to the local charge density by the Poisson equation

$$\nabla^2\psi(z) = -\frac{e}{\varepsilon_0\varepsilon_r}\sum Z_i\rho_i(z) \quad (4)$$

with the following boundary conditions

$$\psi(0) = \psi(D) = \psi_0. \quad (5)$$

As discussed below, the surface potential, ψ_0, depends on the protonation/deprotonation reactions at the surface of porous silica.

To solve Eqs.(3-5) numerically, we start with an initial guess of the ionic density profiles,

$\rho_i(z) = \rho_i^0$. The local excess chemical potential for each ionic species and the local electrical potential, $\Delta\mu_{ex}^i(z)$ and $\psi(z)$, are then calculated from the initial density profiles and the Poisson equation with known electric potentials at the boundaries. Next, a new set of ionic density profiles are obtained from Eq. (3), and the numerical procedure repeats unit convergence ($\left|\frac{\Delta\rho_i}{\rho_o^i}\right| < 10^{-3}$ at all positions). From the ion distributions and the electrical potential, we calculate the surface charge density according to the overall charge neutrality condition

$$Q = -\sum_i Z_i e \int_0^{H/2} dz \rho_i(z). \quad (6)$$

In our CDFT calculations, we assume a layer of surface charge at the surface of the silica nanopore (*viz*., the center of silanol groups) where *z = 0*.

2.3 Surface reaction model

Charge regulation takes place at the silica surface by protonation/deprotonation reactions of the dissociable functional groups [78]:

$$\mathrm{SiOH} \leftrightarrow \mathrm{SiO^-} + \mathrm{H^+} \quad (A)$$

$$\mathrm{SiOH} + \mathrm{H^+} \leftrightarrow \mathrm{SiOH_2^+} \quad (B)$$

Accordingly, the equilibrium constants are

$$K_A = \frac{N_{SiO^-}[H^+]_s}{N_{SiOH}} \text{ and } K_B = \frac{N_{SiOH_2^+}}{N_{SiOH}[H^+]_s} \quad (7)$$

where N_{SiOH}, N_{SiO^-}, and $N_{SiOH_2^+}$ are the number densities of SiOH, $\mathrm{SiO^-}$, and $\mathrm{SiOH_2^+}$ groups at the silica surface, respectively. In Eq.(7), $[H^+]_s$ stands for the proton concentration at the silica interface. Neglecting proton interaction with other ionic species in the system, we can predict the surface density of protons from the Boltzmann equation:

$$[H^+]_s = C_{H^+}(z)|_{z=s} = C_1 exp(-\frac{z_i F\psi_0}{RT}) \quad (8)$$

where ψ_0 is the surface electrical potential, C_1 is the bulk concentration of $[H^+]$ ions,

which is related to the solution pH by $\mathrm{pH} = -\log(\mathrm{C_{H^+}})$.

The total number density of silanol functional groups on the solid/liquid interface consists of three contributions:

$$N_{total} = N_{SiOH} + N_{SiO^-} + N_{SiOH_2{}^+} \quad (9)$$

From Eqs. (7) - (9), we can obtain the surface charge density of the silica nanopore

$$Q = F(N_{SiOH_2{}^+} - N_{SiO^-}) = -FN_{total}\frac{K_A - K_B[H^+]_s{}^2}{K_A + [H^+]_s + K_B[H^+]_s{}^2} \quad (10)$$

where $F = 96485\ \mathrm{C/mol}$ is the Faraday constant. The parameters for the silica surface can be found from the literature: $\mathrm{N_{total}} = 2\times10^{-6}\ \mathrm{mol/m^2}$, $\mathrm{pK_A} = -\log(\mathrm{K_A}) = 6.8$ and $\mathrm{pK_B} = -\log(\mathrm{K_B}) = 1.7$.[42,43]

The above procedure can be calibrated with experimental data for charge regulation of open silica surfaces. As shown in Fig. S1, a combination of CDFT and the surface reaction model is able to reproduce the experimental results at different pH and salt concentrations. For an open silica surface, similar results can be accomplished by replacing CDFT with the PB equation. It suggests that our silt pore model can successfully capture the surface charge properties of realistic porous silica. Whereas CDFT and PB yield similar results for this particular set of data, the ion distributions obtained from CDFT calculations can be significantly different from those solved from the PB equation when the pore size is comparable with or smaller than the Debye screening length. For example, Figure S2 shows density profiles for ion distributions in a nanopore. While the PB equation predicts an unrealistic contact density at the surface, CDFT predicts a more reasonable counterion density profile, with the peak position being 0.15 nm to the surface due to the ionic excluded volume effects.

3 Results and discussion

The surface charge of a silica nanopore depends on solution pH as well as ionic distributions. Because neither the surface charge nor the surface electrical potential is known from experiment, an iterative procedure is required to calculate the ionic distributions inside the pore and the surface composition self-consistently (Figure. 1). For all results discussed in the following, we obtain these quantities by solving the EDL and surface-reaction models simultaneously. First, we construct a series of curves for the surface charge density Q versus the surface potential ψ_0 by CDFT calculations at different bulk salt concentrations, as shown schematically by the violet, blue and cyan lines in Figures 1b and 1c. Next, we establish the relations between Q and ψ_0 at different pH values by using the surface-reaction model. These curves are shown as the grey dashed lines in Figures 1b and 1c. Finally, we obtain the surface charge density and the surface electrical potential (viz., zeta potential) at the given pH and the electrolyte concentration.

3.1 pH effects on the surface charge densities of silica nanopores

Because of deprotonation, the surface charge density of a silica surface becomes more negative as the pH increases. Such an effect is expected to be sensitive to both the pore size and salt concentration because the confinement alters the surface electrical potential and the local proton concentration. As shown in Figure 2, the surface charge density becomes more negative as pH increases, which agrees quantitatively with the experimental result for an open silica surface.[44] The absolute value of the surface charge density declines with the pore size because of the surface-surface interactions. Similar results can be found in previous studies of two planar electrodes, the surface charge will increase upon on the increase of the plate

separation.[45] As expected, the pore size effect is most significant at small salt concentrations because of the long-range electrostatic interactions.

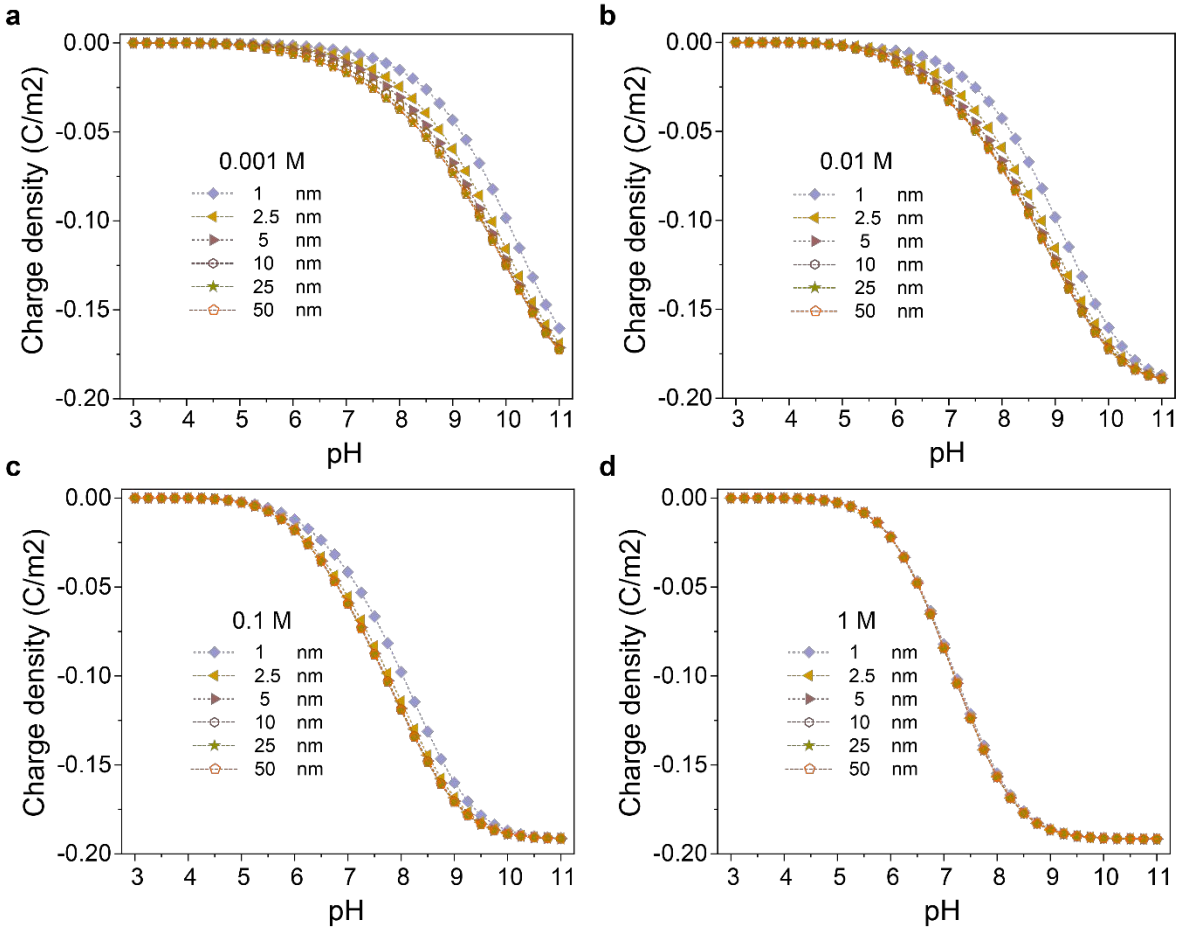

Figure 2. Variation of the surface charge density of silica nanopores of different pore width (legends, 1 nm -50 nm) with pH at different NaCl concentrations, 0.001M (a), 0.01M (b), 0.1M (c), and 1 M (d).

3.2 Salt concentration effects in different nanopores

Figure 3a shows how the salt concentration affects the surface charge densities of different silica nanopores. At the same pH and pore size, the absolute value of the surface charge density increases with the salt concentration because of the electrostatic screening effect. The trend is consistent with the experimental data and other theoretical results for single silica surfaces.[46,47]Take pH = 8 and D = 50 nm, as an example, the surface charge density is about -

0.04 C/m^2 for $C_{NaCl} =$ 0.001 M, while it is increased to -0.16 C/m^2 for $C_{NaCl} = 1$ M.

The salt concentration affects the surface charge density of silica nanopore by altering the proton concentration at the surface. As shown in Figure 3b, the proton concentration at the surface falls as C_{NaCl} increases, suggesting that H^+ ions are excluded from the surface because of the reduction of the surface electrical potential (Figure 3c). In other words, a lower surface H^+ concentration leads to more deprotonation of the silica surface thus more negative charge. When the pore size of a silica nanopore increases from 1 nm to 50 nm in 0.001 M NaCl, the proton concentration is reduced accordingly from 1.76×10^{-6} M to 6.35×10^{-7} M. It is worth noting that the surface concentration of H^+ ions varies more significantly with the pore size at low salt concentrations (Figure 3b). Again, the pore size effect is most significant at low salt concentrations.

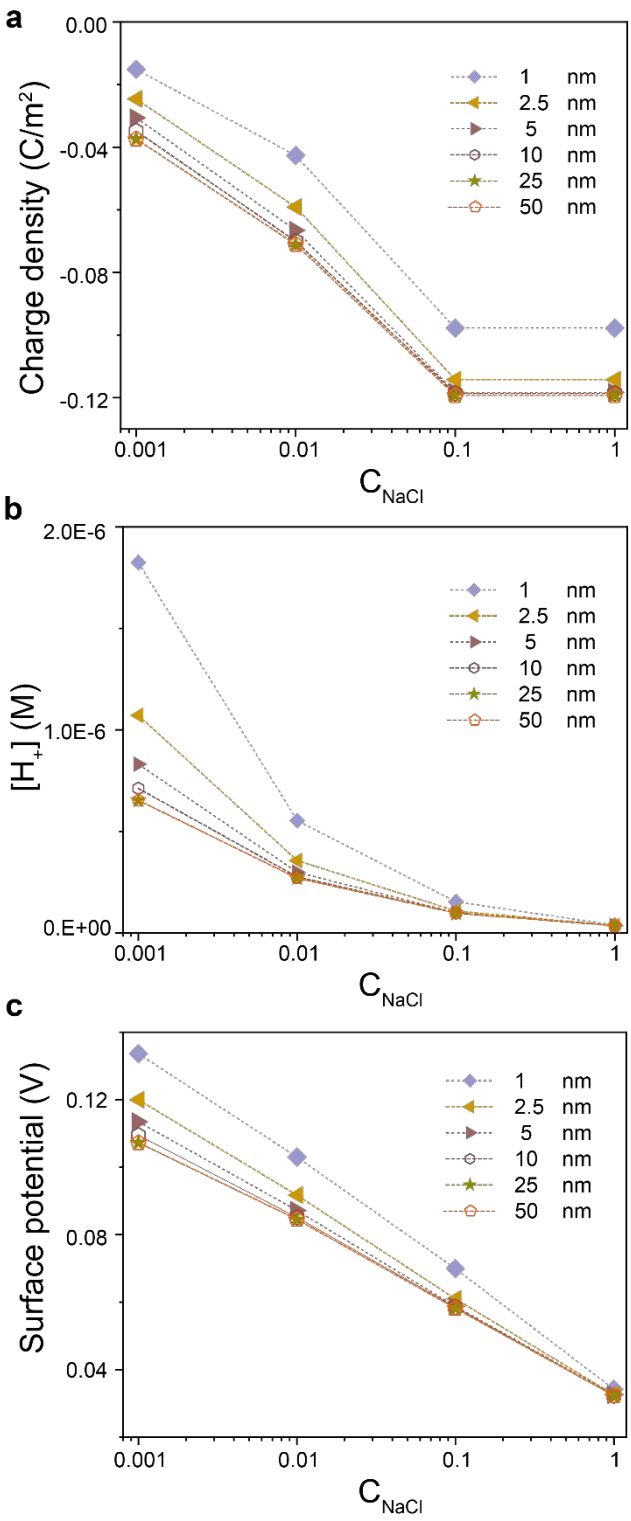

Figure 3. Variation of the surface charge density (a), the surface proton concentration (b), and the surface potential (c) with C_{NaCl} at different pore sizes. In all cases, pH = 8 and the different pore sizes are shown with different markers.

3.2 The pore size effects on ionic screening

From the above discussions, we see that the pore size plays a vital role in determining the surface charge density of a silica nanopore at high pH and low salt concentrations. At all pH values and different salt concentrations, the absolute value of the surface charge density decreases with the pore width (Figure 2) because of the increased proton concentration at the surface (Figure 3b). The surface charge density approaches an asymptotic limit when the pore size is sufficiently large, i.e., when the EDLs from the opposite surfaces of the slit pore are independent. In other words, the pore size effect becomes less important when it is larger than a critical value that depends on both the pH and salt concentration. For instance, at pH = 8, the critical pore size is about 25 nm at C_{NaCl} = 0.001 M, while it is about 1 nm at C_{NaCl} = 1 M. The lower of the salt concentration, the larger the critical pore value.

As well known, the Debye screening length, defined as $\lambda_D = \sqrt{\varepsilon_0 \varepsilon_r RT / \sum_i^2 F^2 Z_i^2 C_{i0}}$, provides a measure of the EDL thickness. In nanopores, both the ionic concentrations and the EDL thickness will be influenced by confinement due to overlapped EDL, which has been demonstrated in previous work.[48] To characterize the pore-size effects on ionic screening, we present in Figure 4 the proton concentration and the surface charge density at different pH and salt concentrations. Here the surface charge density is normalized by the asymptotic value approximated by that for a slit pore at D = 50 nm, Q/Q_{50}. For the four electrolyte concentrations considered in this work, the normalized surface charge density increases with the pore size at all pH values. When the pH is fixed (e.g., pH=8), the normalized surface charge densities are close to 1 for D > 25 nm. In this case, the Debye screening length is much smaller than the pore size, explaining a weak influence of the pore size on the surface charge density. Interestingly, the normalized surface charge density reaches the asymptotic limit at a smaller pore size (D <

5 nm) when the pH is increased to 11. For example, the normalized surface charge density is 0.40 for D = 1 nm, C_{NaCl} = 0.001 M at pH = 8 while it is 0.93 at pH = 11. Similar to the explanation above, the extent of EDL overlap is relatively insignificant when pH = 11 compared with pH = 8 so that the effects of pore size on surface charge is less evident. \

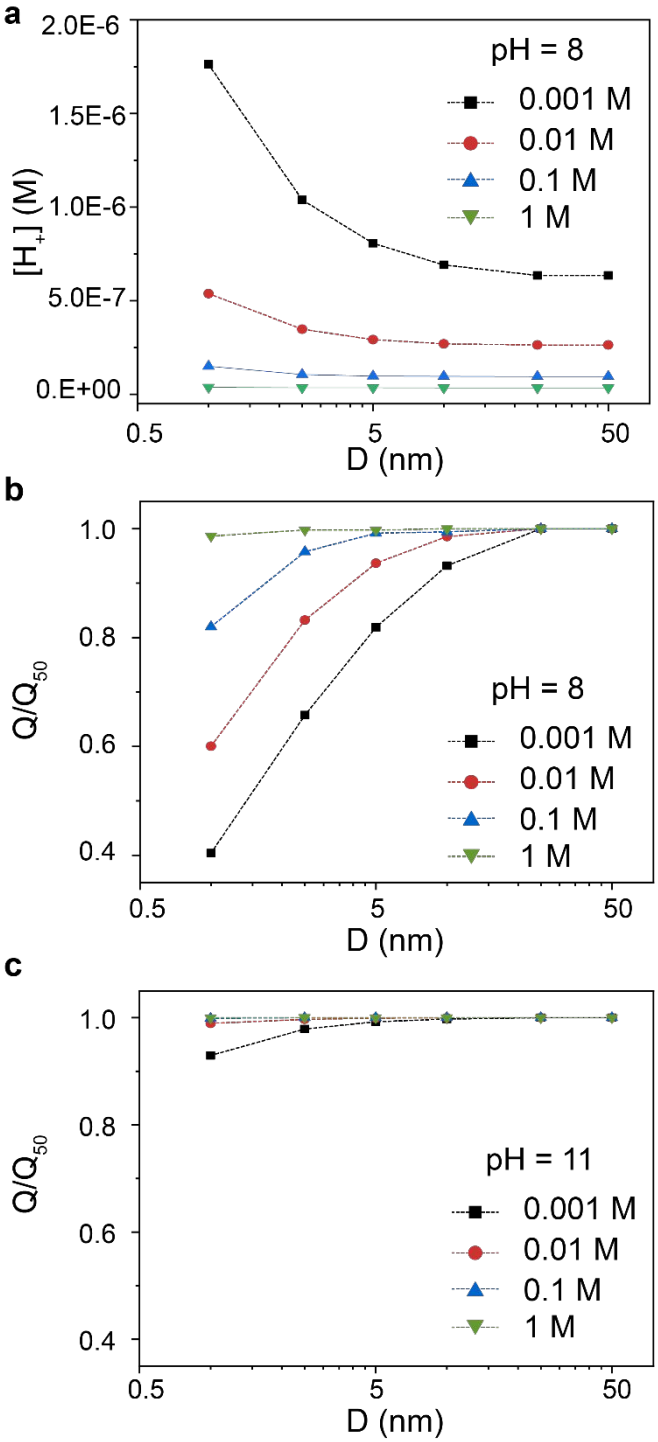

Figure 4. Surface proton concentration versus pore size at pH = 8 (a) and the normalized

241 surface charge density of a silica nanopore as a function of the pore size at pH = 8 (b) and 11
242 (c). The legends denote different NaCl concentrations.

243 To investigate the combined effects of the pore size (D) and the electrolyte concentration
244 on the surface charge density of silica nanopores, we further consider the surface charge density
245 as a function of the reduced Debye length, λ_D/D. This parameter reflecting the EDL overlap
246 has also been used in previous theoretical work (e.g. PNP).[15,28,29] Results show that the large
247 value of λ_D/D significantly causes the surface charge density to deviate from that of an open
248 surface, which aligns to our predictions. As shown in Figure 5, the normalized surface charge
249 density is virtually invariant when the pore size is larger than the Debye length but it declines
250 sharply as the reduced Debye length, λ_D/D, is beyond a critical value that depends on both pH
251 and salt concentration. Interestingly, the reduced surface charge density is close to unity when
252 λ_D/D is smaller than 0.5 regardless of pH and salt concentration. Overall, the surface charge
253 density is weakly correlated with the silica nanopore size when $D > 2\lambda_D$, while it becomes
254 more sensitive to the pore size when $D < 2\lambda_D$ due to the EDL overlap. Notably, though
255 conventional theoretical works (e.g. PB or PNP) have reported the significant pore size effects
256 on the surface charge density when the pore size is comparable to that of the EDL dimension.
257 In this work, we identified the surface charge regulation of silica nanopore using CDFT when
258 the pore size is similar to the ion diameter as small as 1 nm, where the ion size effect becomes
259 more important and could not be ignored, as shown in Figure S1.We hope that our model would
260 provide more accurate microscopic insights into both the EDL structures inside silica nanopore
261 and the surface properties of the porous silica.

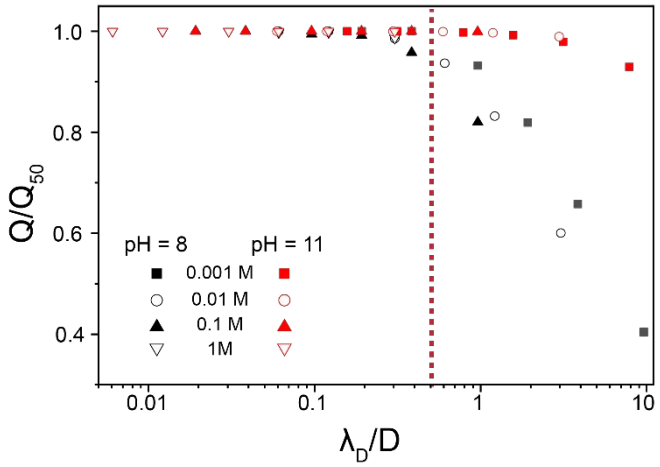

Figure 5. Normalized surface charge density versus the ratio of the Debye length λ_D to the pore size (D). Different symbols represent different electrolyte concentrations, while different colors show different pH values (black for pH = 8; red for pH = 11).

4 Conclusion

In summary, the classical density functional theory (CDFT) is combined with a surface reaction model to predict the pore size effects on the surface charge density of silica nanopores at different pH and NaCl concentrations. At the asymptotic limit of large pores, the theoretical predictions agree well with the experimental data for the surface charge densities corresponding to planar silica surfaces or silica particles. As expected, the surface charge density becomes more negative as the pH increases due to the deprotonation of the SiOH functional groups. The coarse-grained model is able to capture a decrease of H^+ concentration at the surface as the electrolyte concentration increases. Furthermore, the surface charge density increases with the pore size and approaches an asymptotic limit as the EDL overlapping becomes negligible. The pore size effect is less significant at high electrolyte concentration and a large pH value.

Charge regulation for silica nanopores reflects a combined effect of the pore size and

electrolyte concentration as represented by the ratio of the Debye screening length (λ_D) to the nanopore size (D). When the pore size is much larger than the Debye length, the pore size effect on the surface charge density is relatively insignificant regardless of the pH and electrolyte concentration. By contrast, the pore size has a strong influence on the surface charge density when the pore size is close to the Debye screening length. In all cases, the absolute value of the surface charge density decreases as the pore size is reduced. This work demonstrates that a combination of the CDFT and a surface reaction model is able to capture the pore size effects under nanoconfinement. The molecular theory provides insights into the surface properties of silica nanopores useful for their broad practical applications.

Acknowledgment

This research was sponsored by the financial support by the National Natural Science Foundation of China (No. 91834301 and 21808055), China Postdoctoral Science Foundation (2019M651416), and Shanghai Sailing Program (18YF1405400, 19YF1411700). J.W. thanks the financial support from the Fluid Interface Reactions, Structures and Transport (FIRST) Center, an Energy Frontier Research Center funded by the U.S. Department of Energy, Office of Basic Energy Sciences.

REFERENCES

1 Y. Wang and H. Gu, Core–Shell-Type Magnetic Mesoporous Silica Nanocomposites for Bioimaging and Therapeutic Agent Delivery, *Adv. Mater.,* 2015, **27**, 576–585.

2 Z. Wang, Y. Liu, L. Yu, Y. Li, G. Qian and S. Chang, Nanopipettes: a potential tool for DNA detection, *Analyst*, 2019, **144**, 5037–5047.

3 X. He, K. Zhang, Y. Liu, F. Wu, P. Yu and L. Mao, Chaotropic Monovalent Anion-Induced

Rectification Inversion at Nanopipettes Modified by Polyimidazolium Brushes, *Angew. Chem.,* 2018, **130**, 4680–4683.

4 S. J. Kim, G. Chase and S. C. Jana, The role of mesopores in achieving high efficiency airborne nanoparticle filtration using aerogel monoliths, *Sep. Pur. Technol.*, 2016, **166**, 48–54.

5 W. Li, J. Liu and D. Zhao, Mesoporous materials for energy conversion and storage devices, *Nat. Rev. Mat.*, 2016, **1**, 16023.

6 J. Liang, Z. Liang, R. Zou and Y. Zhao, Heterogeneous Catalysis in Zeolites, Mesoporous Silica, and Metal–Organic Frameworks, *Adv. Mater.,* 2017, **29**, 1701139.

7 D. A. Sverjensky and N. Sahai, Theoretical prediction of single-site surface-protonation equilibrium constants for oxides and silicates in water, *Geochim. Cosmochim. Acta*, 1996, **60**, 3773–3797.

8 S. H. Behrens and D. G. Grier, The charge of glass and silica surfaces, *J. Chem. Phsy.,* 2001, **115**, 6716–6721.

9 M. Nyström, A. Pihlajamäki and N. Ehsani, Characterization of ultrafiltration membranes by simultaneous streaming potential and flux measurements, *J. Membr. Sci.*, 1994, **87**, 245–256.

10 T. Jimbo, M. Higa, N. Minoura and A. Tanioka, Surface Characterization of Poly(acrylonitrile) Membranes Graft-Polymerized with Ionic Monomers As Revealed by ζ Potential Measurement, *Macromolecules*, 1998, **31**, 1277–1284.

11 T. Jimbo, A. Tanioka and N. Minoura, Characterization of an Amphoteric-Charged Layer Grafted to the Pore Surface of a Porous Membrane, *Langmuir*, 1998, **14**, 7112–7118.

12 C. Causserand, M. Nyström and P. Aimar, Study of streaming potentials of clean and

fouled ultrafiltration membranes, *Journal of Membrane Science*, 1994, **88**, 211–222.

13 M. R. Teixeira, M. J. Rosa and M. Nyström, The role of membrane charge on nanofiltration performance, *J. Membr. Sci.*, 2005, **265**, 160–166.

14 M. Jia and T. Kim, Multiphysics Simulation of Ion Concentration Polarization Induced by Nanoporous Membranes in Dual Channel Devices, *Anal. Chem.*, 2014, **86**, 7360–7367.

15 C.-C. Chang, R.-J. Yang, M. Wang, J.-J. Miau and V. Lebiga, Liquid flow retardation in nanospaces due to electroviscosity: Electrical double layer overlap, hydrodynamic slippage, and ambient atmospheric CO2 dissolution, *Phys. Fluids*, 2012, **24**, 072001.

16 R. P. Abendroth, Surface charge development of porous silica in aqueous solution, *J. Phys. Chem*, 1972, **76**, 2547–2549.

17 M. Karlsson, C. Craven, P. M. Dove and W. H. Casey, Surface Charge Concentrations on Silica in Different 1.0 M Metal-Chloride Background Electrolytes and Implications for Dissolution Rates, *Aquat. Geochem.*, 2001, **7**, 13–32.

18 A. Salis, D. F. Parsons, M. Boström, L. Medda, B. Barse, B. W. Ninham and M. Monduzzi, Ion Specific Surface Charge Density of SBA-15 Mesoporous Silica, *Langmuir*, 2010, **26**, 2484–2490.

19 D. C. Martínez Casillas, M. P. Longinotti, M. M. Bruno, F. Vaca Chávez, R. H. Acosta and H. R. Corti, Diffusion of Water and Electrolytes in Mesoporous Silica with a Wide Range of Pore Sizes, *J. Phys. Chem.*, 2018, **122**, 3638–3647.

20 H. Rho, K. Chon and J. Cho, Surface charge characterization of nanofiltration membranes by potentiometric titrations and electrophoresis: Functionality vs. zeta potential, *Desalination*, 2018, **427**, 19–26.

345 21 C. Lian, X. Kong, H. Liu and J. Wu, Flow effects on silicate dissolution and ion transport
346 at an aqueous interface, *Phys Chem Chem Phys*, 2019, **21**, 6970–6975.
347 22 H. Daiguji, P. Yang and A. Majumdar, Ion Transport in Nanofluidic Channels, *Nano Lett.*,
348 2004, **4**, 137–142.
349 23 H. Daiguji, P. Yang, A. J. Szeri and A. Majumdar, Electrochemomechanical Energy
350 Conversion in Nanofluidic Channels, *Nano Lett.*, 2004, **4**, 2315–2321.
351 24 A. P. Thompson, Nonequilibrium molecular dynamics simulation of electro-osmotic flow
352 in a charged nanopore, *J. Chem. Phys.,* 2003, **119**, 7503–7511.
353 25 R. Qiao and N. R. Aluru, Charge inversion and flow reversal in a nanochannel electro-
354 osmotic flow, *Phys. Rev. Lett.*, 2004, **92**, 198301.
355 26 R. Qiao and N. R. Aluru, Surface-charge-induced asymmetric electrokinetic transport in
356 confined silicon nanochannels, *Appl. Phys. Lett.*, 2005, **86**, 143105.
357 27 M. Wang and S. Chen, Electroosmosis in homogeneously charged micro- and nanoscale
358 random porous media, *J Colloid Interface Sci.*, 2007, **314**, 264–73.
359 28 S. Tumcan and B. Murat, Size Dependent Surface Charge Properties of Silica Nano-
360 Channels: Double Layer Overlap and Inlet/Outlet Effects, *Phys. Chem. Chem. Phys.*, 2016, **18**,
361 21–46.
362 29 T. Sen and M. Barisik, Internal surface electric charge characterization of mesoporous
363 silica, *Sci. Rep.*, 2019, **9**, 137.
364 30 C. Lian, H. Su, C. Li, H. Liu and J. Wu, Non-Negligible Roles of Pore Size Distribution
365 on Electroosmotic Flow in Nanoporous Materials, *ACS Nano*, 2019, **13**, 8185–8192.
366 31 R. B. Schoch, J. Han and P. Renaud, Transport phenomena in nanofluidics, *Rev. Mod.*

Phys., 2008, **80**, 839–883.

32 D. E. Jiang, Z. Jin and J. Wu, Oscillation of capacitance inside nanopores, *Nano Lett.*, 2011, **11**, 5373–7.

33 C. Lian, D. Jiang, H. Liu and J. Wu, A Generic Model for Electric Double Layers in Porous Electrodes, *J. Phys. Chem. C*, 2016, **120**, 8704–8710.

34 D. E. Jiang and J. Wu, Unusual effects of solvent polarity on capacitance for organic electrolytes in a nanoporous electrode, *Nanoscale*, 2014, **6**, 5545–50.

35 C. Lian, K. Liu, K. L. Van Aken, Y. Gogotsi, D. J. Wesolowski, H. L. Liu, D. E. Jiang and J. Z. Wu, Enhancing the Capacitive Performance of Electric Double-Layer Capacitors with Ionic Liquid Mixtures, *ACS Energy Lett.*, 2016, **1**, 21–26.

36 C. Lian, H. Liu, C. Li and J. Wu, Hunting ionic liquids with large electrochemical potential windows, *AIChE J.,* 2019, **65**, 804–810.

37 D. Gillespie, D. N. Petsev and F. van Swol, Electric Double Layers with Surface Charge Regulation Using Density Functional Theory, *Entropy*, 2020, **22**, 132.

38 Y. X. Yu, J. Wu and G. H. Gao, Density-functional theory of spherical electric double layers and zeta potentials of colloidal particles in restricted-primitive-model electrolyte solutions, *J Chem. Phys.*, 2004, **120**, 7223–33.

39 Y.-X. Yu and J. Wu, Structures of hard-sphere fluids from a modified fundamental-measure theory, *J. Chem. Phys.*, 2002, **117**, 10156–10164.

40 B. Tansel, J. Sager, T. Rector, J. Garland, R. F. Strayer, L. Levine, M. Roberts, M. Hummerick and J. Bauer, Significance of hydrated radius and hydration shells on ionic permeability during nanofiltration in dead end and cross flow modes, *Sep. Pur. Technol.*, 2006,

51, 40–47.

41 M. Addicoat, R. Atkin, J. N. Canongia Lopes, M. Costa Gomes, M. Firestone, R. Gardas, S. Halstead, C. Hardacre, L. J. Hardwick, J. Holbrey, P. Hunt, V. Ivanistsev, J. Jacquemin, R. Jones, B. Kirchner, R. Lynden-Bell, D. MacFarlane, G. Marlair, H. Medhi, M. Mezger, A. Padua, I. Pantenburg, S. Perkin, J. Reid, M. Rutland, S. Saha, K. Shimizu, J. M. Slattery, M. Swadzba-Kwasny, S. Tiwari, S. Tsuzuki, B. Uralcan, A. van den Bruinhorst, M. Watanabe and J. Wishart, Structure and dynamics of ionic liquids: general discussion, *Faraday Discuss.*, 2018, **206**, 291–337.

42 M. B. Andersen, J. Frey, S. Pennathur and H. Bruus, Surface-dependent chemical equilibrium constants and capacitances for bare and 3-cyanopropyldimethylchlorosilane coated silica nanochannels, *J. Colloid Interface Sci.*, 2011, **353**, 301–310.

43 M. Barisik, S. Atalay, A. Beskok and S. Qian, Size Dependent Surface Charge Properties of Silica Nanoparticles, *J. Phys. Chem. C*, 2014, **118**, 1836–1842.

44 J. Sonnefeld, M. Löbbus and W. Vogelsberger, Determination of electric double layer parameters for spherical silica particles under application of the triple layer model using surface charge density data and results of electrokinetic sonic amplitude measurements, *Colloids Surf., A*, 2001, **195**, 215–225.

45 M. Polat and H. Polat, Analytical solution of Poisson?Boltzmann equation for interacting plates of arbitrary potentials and same sign, *J. Colloid Interface Sci.*, 2010, **341**, 178–185.

46 Z. Ovanesyan, A. Aljzmi, M. Almusaynid, A. Khan, E. Valderrama, K. L. Nash and M. Marucho, Ion-ion correlation, solvent excluded volume and pH effects on physicochemical properties of spherical oxide nanoparticles, *J Colloid Interface Sci.*, 2016, **462**, 325–33.

47 S. Atalay, M. Barisik, A. Beskok and S. Qian, Surface Charge of a Nanoparticle Interacting with a Flat Substrate, *J. Phys. Chem. C*, 2014, **118**, 10927–10935.

48 W. Qu and D. Li, A Model for Overlapped EDL Fields, *Journal of Colloid and Interface Sci*, 2000, **224**, 397–407.